

Core–Shell Poly(allyamine hydrochloride)-Pyrene Nanorods Decorated with Gold Nanoparticles

Zhipeng Wang,^{†,‡} Andre G. Skirtach,[‡] Yang Xie,[†] Mengying Liu,[†] Helmuth Möhwald,[‡] and Changyou Gao^{*,†}

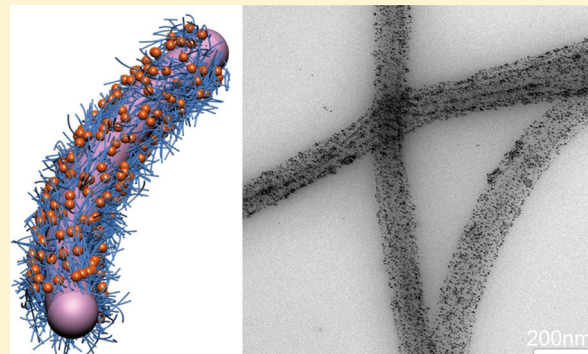
[†]MOE Key Laboratory of Macromolecular Synthesis and Functionalization, Department of Polymer Science and Engineering, Zhejiang University, Hangzhou 310027, China

[‡]Max Planck Institute of Colloids and Interfaces, Research Campus Golm, 14424 Potsdam, Germany

Supporting Information

ABSTRACT: Water-dispersible and fluorescent core–shell nanorods (NRs) consisting of covalently linked poly(allyamine hydrochloride)-pyrene (PAH-Py) were synthesized and used for fabricating hybrid organic–inorganic NRs. The reaction between 1-pyrenecarboxaldehyde (Py-CHO) nanorods and PAH was driven by Schiff base formation and followed by NaBH₄ reduction, and caused 28% mass loss of Py molecules at the final stage (2 h). The final PAH-Py NRs contained 42% PAH, corresponding to a Py substitution ratio of 34.5%. They were uniform in size with a Py-CHO core (81.2 ± 16.4 nm) and PAH shell (45.0 ± 8.8 nm) fibrillar structure, and had a surface zeta potential of 53.7 ± 5.1 mV. The PAH-Py NRs could survive after annealed at 80°C or dispersed in ethanol, and showed good suspension stability in water. Because of the functional amino groups, the nanorods could act as nanoanchors to immobilize either positively or negatively charged gold nanoparticles, or as nanoreactors to synthesize gold and platinum nanoparticles *in situ*. Very small quenching of the fluorescence was achieved due to the isolation effect of the PAH layer. The method described here provides a new approach for modifying organic surfaces with nanoparticles and endowing them with multiple functions.

KEYWORDS: pyrene, nanorods, hybrids, poly(allyamine hydrochloride), gold nanoparticles



INTRODUCTION

One-dimensional (1D) nanostructure materials such as nanowires, nanorods and nanotubes have attracted increasing interest in the thriving field of nanoscience and nanotechnology,^{1–6} mainly because of their unique photoelectronic, magnetic and biological properties determined by their size and 1D shape. There are numerous potential applications of 1D nanostructure materials as building blocks for electronic,^{7–9} optoelectronic,^{10–12} and electrochemical nanodevices;^{13–15} biological nanosensor;⁶ templates for hybrid hierarchical nanoarchitecture;^{3,16} and other enhanced functional materials. The well-developed 1D inorganic nanomaterials possess high efficiency of electron transportation, fluorescence, catalysis, and so on.^{2,5} Their counterparts, the 1D organic nanomaterials, however, not only display some similar properties but also possess the merits of molecular variety, high flexibility and low cost of materials fabrication, and ease in functionalization. Integration of the advantages of these two types of materials is thereby able to generate hybrid nanomaterials with new structures, properties, and functions in a synergistic way.³

Currently, several approaches have been reported to fabricate the 1D organic nanomaterials, among which the molecular self-assembly is one of the most effective and widely applied

approaches due to its broad adaptation. For instance, planar, rigid aromatic organic molecules and conjugated polymers can self-assemble into 1D nanostructures, mainly through π – π stacking interaction in organic solvents.^{17–20} Amino acids and polypeptides can self-organize to nanofibres and nanowires based on hydrogen bonding or electrostatic interaction.^{21,22} Also, cyclodextrin-covered dendron nanotubes are obtained by a host–guest supramolecular self-assembly process.^{23,24} In addition, polyelectrolytes with electrostatic interaction can be fabricated into nanotubes by depositing multilayers on the channel surface of macroporous template materials (later removing them) via a layer-by-layer assembly method.^{6,25,26} Finally, by constructing the side chains of cylinder polymer brushes through living polymerization, organo-silica hybrid nanowires with a core–shell structure have been built up.^{27,28} Although these methods have prepared nanomaterials with unique properties and potential applications, the pursuit of fabricating multifunctional 1D nanomaterials with more convenience and lower cost will be continued.

Received: June 16, 2011

Revised: September 14, 2011

Published: October 17, 2011

Very recently, we discovered an intriguing phenomenon of protrusion of one-dimensional nanorods (NRs) from poly(allylamine hydrochloride) (PAH)-graft-pyrene (Py) micro-capsules.²⁹ The NRs was composed of 1-pyrenecarboxaldehyde (Py-CHO) (Py-CHO NR) and could be generally obtained through $\pi-\pi$ stacking self-assembly by hydrolysis of Schiff base bonds between PAH and Py-CHO in weak acid solution. Although the as-prepared Py-CHO NRs showed excellent fluorescent property due to the intrinsic nature of Py, the strong hydrophobicity of Py resulted in sedimentation in aqueous solution and thereby the difficulty of further modification.

In this work, a simple but crucial strategy is suggested to solve this problem and endow the Py-CHO NRs with multiple functions. As shown in Scheme 1, the Py-CHO NR is in situ

modified with PAH by reformation of Schiff base bond between PAH and Py-CHO in an alkaline solution, followed by Au or Pt NPs decoration. The well dispersed AuNPs or PtNPs containing PAH-Py NRs are expected to find diverse applications in surface-enhanced Raman spectroscopy (SERS),³⁰ photothermal therapy,³¹ and catalysis.³² The controllable and reversible hydrolysis and synthesis of Schiff base as well as the functionalization of the NRs match well the idea “introduction of reversible bonds into molecules, leads to the emergence of a constitutional dynamic chemistry” from J.-M. Lehn.³³ This strategy can also be extended to fabricating other functional nanomaterials by using different molecules and NPs.

EXPERIMENTAL SECTION

Materials. Poly(allylamine hydrochloride) (PAH, $M_n \sim 70$ kDa), 1-pyrenecarboxaldehyde (Py-CHO), AuNPs with citrate as ligands (AuNP-COOH with a mean particle size of 3.0–5.5 nm and a concentration of 8×10^{12} nanoparticles/mL), hydrogen tetrachloroaurate (III) ($\text{HAuCl}_4 \cdot 3\text{H}_2\text{O}$), potassium platinum(II) chloride (K_2PtCl_4), and azobenzoic acid were purchased from Sigma-Aldrich. AuNPs with 4-(dimethylamino)pyridine as ligands (AuNPs-DMAP with a mean particle size of 8–10 nm and a concentration of 3×10^{14} nanoparticles/mL) was synthesized as reported previously.³⁴ Hydrochloride (HCl) solution (1 mol/L) was purchased from Merck Company and diluted to a desired concentration. Other chemicals

Scheme 1. Fabrication Process of Hybrid NR from Py-CHO NR, PAH, and Metal Nanoparticles or Precursory Chemicals

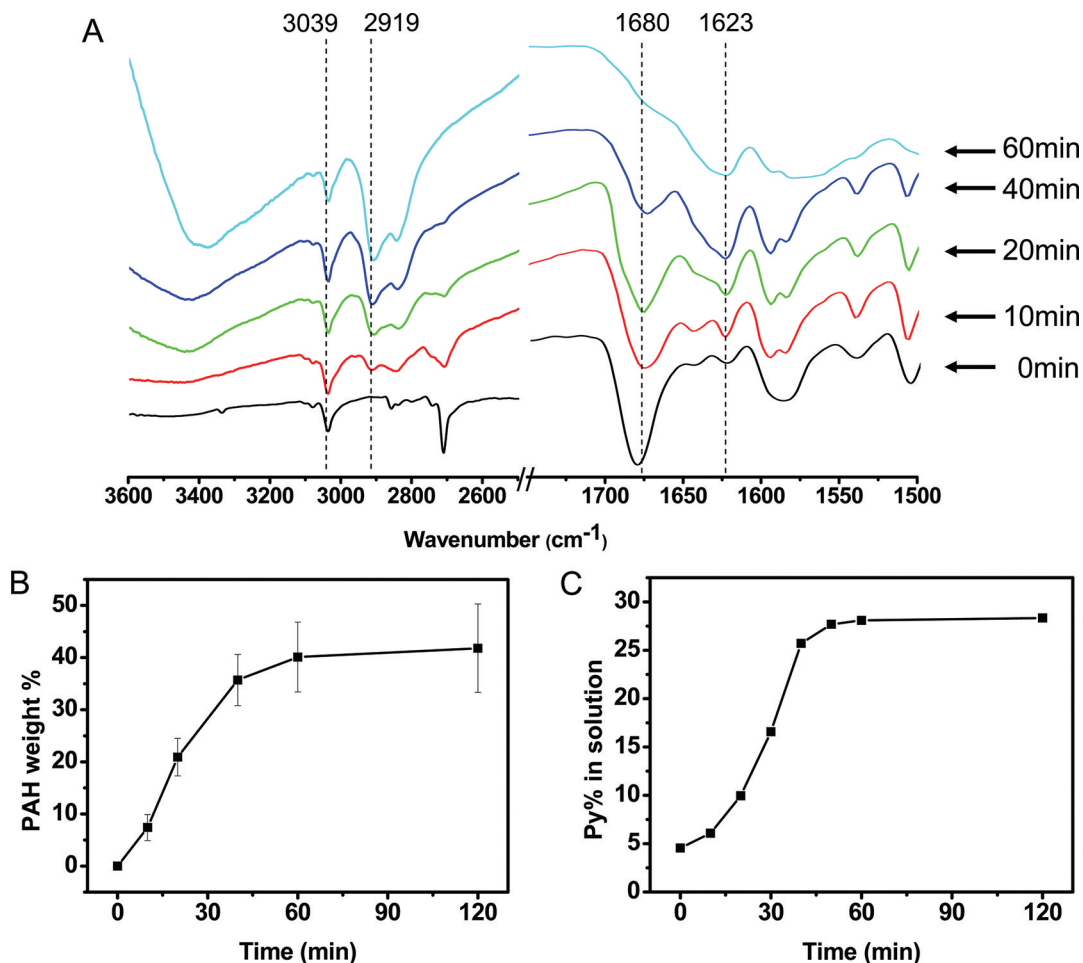
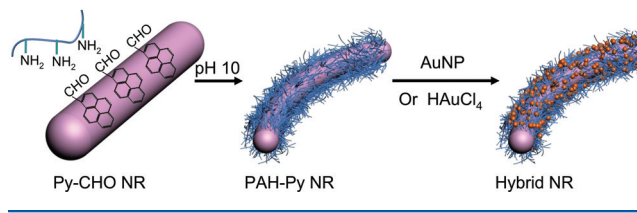


Figure 1. (A) FTIR spectra of the Py-CHO NRs before and after reaction with PAH for different time. The aldehyde group and Schiff base appear at 1680 and 1623 cm^{-1} , respectively. The peaks at 3039 and 2919 cm^{-1} are assigned to pyrene and methylene groups, respectively. (B) PAH weight percentage on the Py-CHO NRs as a function of time. (C) The released amount of Py-CHO in PAH solution as a function of time.

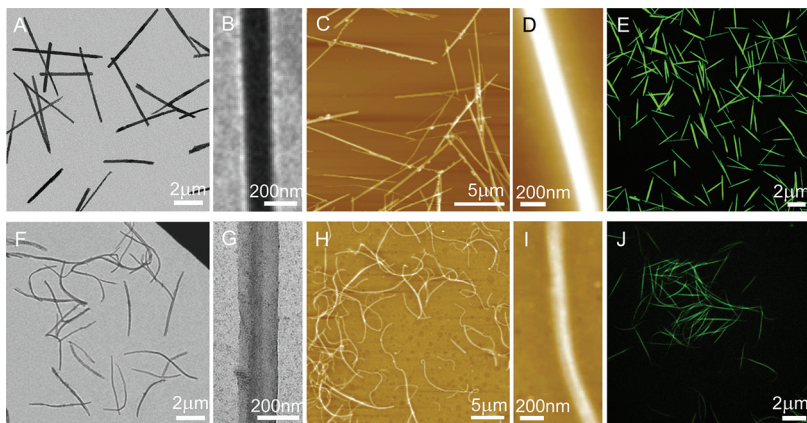


Figure 2. (A, B, F, G) TEM, (C, D, H, I) AFM, and (E, J) CLSM images of Py-CHO NR at (A–E) pH 2 and (F–J) PAH-Py NR at pH 10.

were used as received. The water used in all experiments was prepared via a Millipore Milli-Q purification system and had a resistivity higher than $18 \text{ M}\Omega \text{ cm}$.

The PAH-Py NRs. Py-CHO NRs were fabricated by hydrolysis of Schiff base bonds in PAH-Py polymer at pH 2 within 1 h.²⁹ The as-prepared 50 mL suspension of NRs was adjusted to pH 10 by adding 0.11 mL 5 M NaOH solution. After 2 h, 5 mL of freshly prepared ice cold NaBH₄ aqueous solution (20 g/L) was added dropwise within 30 min. After 6 h, the reaction mixture was purified by ultrafiltration to remove excessive reagents and free salts. The suspension of PAH-Py NR was then kept at 4 °C in water for further use.

Preparation of AuNP-COOH- and AuNP-DMAP-Modified PAH-Py NRs. An aqueous solution containing 20 μL of AuNP-COOH or AuNP-DMAP (whose concentration was diluted to 8×10^{12} nanoparticles/mL, same as that of the AuNP-COOH) was mixed with 50 μL of PAH-Py NR (0.01 mg/mL) for sufficient binding between PAH and AuNPs. The obtained products were kept at 4 °C in water for further use.

Synthesis of AuNP on PAH-Py NR. An aqueous solution containing 20 μL of HAuCl₄ (0.4 mM) and 50 μL of PAH-Py NRs (0.01 mg/mL) was gently stirred at 25 °C for 2 days and at 80 °C for 1 h, respectively, to reduce the Au salt to the NPs.

Characterizations. Transmission electron microscopy (TEM) images were obtained with a Zeiss EM 912 Omega microscope at an acceleration voltage of 120 kV. A 3 μL droplet of a dilute suspension (0.005 g/L) was deposited onto a copper grid (200 mesh) with a carbon film, followed by drying in vacuum. The statistical analysis of NRs size was performed using the Image J program. In each case, at least 50 objects were measured. Atomic force microscopy (AFM) images were recorded with a Nanoscope IIIa multimode microscope (Digital Instruments Inc., Santa Barbara, CA). Confocal laser scanning microscopy (CLSM) images were taken on a LEICA TCS system (Aristoplan, Germany, 100 × oil immersion using commercial software). The samples were prepared by casting the as-prepared solutions on freshly cleaved mica (for AFM) and glass slide (for CLSM), respectively. Fourier transform infrared spectroscopy (FTIR) was measured on a Bruker Equinox 55/S using a KBr pellet. The NRs were separated from solution by membrane filtration at different reaction time and dried in vacuum before measurement. Elemental analysis was carried out by Flash EA-1112. UV-vis spectra were taken by a Cary 4E UV-visible spectrophotometer. Steady-state fluorescence spectra were measured on a Fluoromax-4 spectrophotometer (Horiba, Jobin Yvon). Zeta potential was measured on a Malvern Zetasizer Nano ZS instrument. Raman spectroscopy was recorded by a Nicolet-ALMERA FT-Raman spectrometer ($\lambda=785 \text{ nm}$) with 5 cm⁻¹ resolution. After the PAH-Py NRs either modified with AuNPs-COOH modified or not were incubated in trans-azobenzoic acid (0.05 mg/mL) solution for 1 h, they were purified by membrane filtration with sufficient washing to remove the free dye molecules.

RESULTS AND DISCUSSION

The Py-CHO NRs were fabricated by hydrolysis of PAH-Py polymer with a Py substitution degree of 9.4% in pH 2 solution. They had an average length of ~10 μm and width of ~200 nm.²⁹ To improve the colloidal stability and impart multifunctions to the Py-CHO NRs, surface decoration was implemented by reformation of the Schiff base between PAH (Initially existed in the suspension as a result of hydrolysis of PAH-Py) and Py-CHO NRs at pH 10. During the 1 h reaction, the translucent Py-CHO NR solution became gradually clear and the light yellow color was faded concurrently (see Figure S1 in the Supporting Information).

The reformation process of Schiff base was monitored by FTIR spectra (Figure 1A) after the NRs were purified by membrane filtration to remove soluble molecules and small particles. At the original state, the Py-CHO NRs contained only Py-CHO and showed strong aldehyde adsorption at 1680 cm⁻¹ and specific C–H vibration of Py structure at 3039 cm⁻¹ (black line). Along with the development of the reaction, a new absorption at 1623 cm⁻¹ which is assigned to the C=N adsorption appeared and its strength increased gradually, accompanying with weakening and eventual disappearance of 1680 cm⁻¹. Meanwhile, the adsorption peaks at 2912 and 2846 cm⁻¹ (assigned to the –CH₂ group) and 3440 cm⁻¹ (assigned to the –NH₂ group) appeared and were strengthened. All the results confirm the successful anchorage of PAH onto the NRs. No free Py-CHO molecules could be extracted from the PAH-Py NRs by their good solvent ethanol, proving complete transformation of the Py-CHO NRs to the PAH-Py NRs after 1 h.

Elemental analysis found that the PAH weight percentage in the NRs increased mainly in the first 1 h to approximately 40.1% and ended with 41.8% at 2 h (Figure 1B). The Py-CHO weight percentage, 59.2%, was much higher than that (26.1%) could be reached in a solution reaction between Py-CHO and PAH. This value corresponds to a Py-CHO substitution degree in PAH of 34.5%, which is about 3 times higher than that of PAH-Py synthesized in solution (9.4%). The higher substitution degree may attribute to the larger surface area of the Py-CHO NRs, on which once some –NH₂ groups are anchored the adjacent ones in the same PAH chain have a larger chance to react.

The Py-CHO molecules were found in the filtrate of PAH-Py NRs by UV-vis (see Figure S2 in the Supporting Information), whose amount increased rapidly with the reaction time before

40 min (Figure 1C) and showed a similar regime as that of the PAH weight percentage. The dissolved Py-CHO amount reached to 28.3 wt % at 2 h. FTIR characterization confirmed the formation of PAH-Py polymer in the filtrate, whose substitution degree was 9.8% according to elemental analysis. The lower substitution degree makes the PAH-Py polymer dispersible in water. Therefore, the modification process changed not only the chemical structure but also the molecular organizing way in the nanomaterials. However, no evidence to show that the M_w of PAH had apparent influence, because PAH with a smaller M_w of 15 kDa obtained similar results.

The obtained PAH-Py NRs at 2 h were further reduced by NaBH₄ (confirmed by FTIR in Figure S3 of the Supporting Information) to stabilize their structure. Figure 2A shows that the Py-CHO NRs had a straight and rigid rod-like shape. The PAH-Py NRs, however, became curved and flexible (Figure 2E and Figure S4 in the Supporting Information), which had a dark core (81.2 ± 16.4 nm in diameter) and light shell (45.0 ± 8.8 nm in thickness) structure (Figure 2F) compared to the homogeneous Py-CHO NRs (Figure 2B). The total diameter of the two types of NRs (~170 nm) was very similar. This morphology was substantiated by AFM characterization (Figure 2C, D, G, H). However, the height of the PAH-Py NRs (52.2 ± 5.8 nm) was about one-third of that of the Py-CHO NRs (146 ± 7.3 nm), indicating that the collapse of PAH-Py NRs was due to their softer PAH shells. The NRs were visible under CLSM due to the fluorescent emission of pyrene, but the relative intensity of PAH-Py NRs (Figure 2I) was slightly weaker than that of the Py-CHO NRs (Figure 2E). Therefore, the Py-CHO NRs were covalently covered with a PAH layer to obtain the PAH-Py NRs, which showed a more flexible and curved structure likely due to the partial loss of the Py-CHO molecules.

After PAH decoration, the excimer emission peak at 508 nm became broader compared with that of the Py-CHO NRs (see Figure S5 in the Supporting Information), and showed a 30% decrease in fluorescence intensity as a result of Py-CHO loss. The monoclinic crystal structure of the Py-CHO NRs disappeared after formation of the PAH-Py NRs, which was determined as an amorphous state (see Figure S6 in the Supporting Information). The reduction of the Schiff base, on the other hand, stabilized the chemical structure of the PAH-Py NRs. For example, the reduced PAH-Py NRs could not be decomposed again in acidic solution (see Figure S7B in the Supporting Information) as that of their unreduced counterparts (see Figure S7A in the Supporting Information), which reformed the straight Py-CHO NRs again. The PAH-Py NRs could survive after annealed at 80 °C or dispersed in ethanol (see Figure S7C, D in the Supporting Information).

The PAH decoration significantly improved the suspension stability of the nanorods. The freshly prepared Py-CHO NRs changed quickly from a stable dispersion (Figure 3A1) to flocculation and precipitation in water within 3–5 days (Figure 3A2). However, the PAH-Py NRs (Figure 3B1) were still dispersed homogeneously even after 3 months of storage (Figure 3B2) because of the surface charge repulsion (zeta potential: 53.7 ± 5.1 mV). The PAH-Py NRs were precipitated at pH 13 (Figure 3C1) as a result of charge neutralization, but could be well resuspended again when the solution was readjusted to pH 6 (Figure 3C2).

The composite structure of PAH-Py NRs provides the ease of multiple choices for further modification to obtain functional nanomaterials, since the amino group has high reactivity with

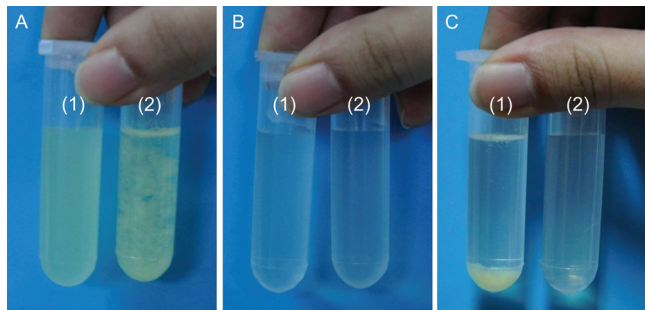


Figure 3. Photographs of (A) Py-CHO NRs solution of freshly prepared (1) and 4 days later (2); (B) PAH-Py NRs solution of freshly prepared (1) and 3 months later (2); (C) PAH-Py NRs solution at pH 13 (1) and after readjusted to pH 6 (2).

carboxyl acid and aldehyde groups, and thereby proteins, DNA, and other functional biomolecules are easily integrated for different biological applications. Furthermore, through electrostatic interaction or ligand complexation the amino groups can also immobilize metal ions or metal nanoparticles such as AuCl₄⁻, PtCl₄²⁻ ions, gold, silver, ZnS, CdS, and TiO₂ nanoparticles to construct 1D organic–inorganic hybrid nanomaterials. Herein, two different approaches were employed to immobilize metal nanoparticles onto the PAH-Py NRs.

The first approach was physical adsorption of preformed gold nanoparticles (AuNPs) capped with either negatively or positively charged ligands. The PAH-Py NRs were incubated in the solution of AuNPs capping with either negatively charged citrate (AuNP-COOH with a mean particle size of 3.0–5.5 nm, zeta potential -30.4 ± 3.2 mV) or positively charged 4-(dimethylamino)pyridine (AuNPs-DMAP with a larger dimension of 8–10 nm, zeta potential 28.8 ± 5.1 mV). Figure 4A and B show that both the AuNP-COOH and AuNPs-DMAP particles were uniformly adsorbed onto/into the PAH-Py NRs, showing an organic/inorganic composite structure. Their weight percentages were found to be 5.6 and 24.7% by EDX, respectively. It is worth mentioning that the cores of the nanorods (even the whole PAH-Py NRs) were hardly distinguishable, because both the Py-CHO core and PAH shell are organic materials and thereby have similar contrast comparing to the Au NPs. The peaks of specific surface plasma absorption were determined at 520 and 533 nm for AuNPs-COOH and AuNPs-DMAP, respectively, which were not changed after adsorption onto the PAH-Py NRs (Figure 4C). When the concentration of AuNPs-DMAP was improved from 8×10^{12} nanoparticles/mL to 3×10^{14} nanoparticles/mL, a larger number of AuNPs-DMAP were found in the PAH-Py NRs (see Figure S8 in the Supporting Information). The irrelevant adsorption of the AuNPs with their surface charge sign should not be governed only by electrostatic attraction²⁴ but also by other forces such as the coordination effect between the amine and Au.³⁵

The fluorescent emission of Py in the PAH-Py NRs was slightly quenched (Figure 4D) to 90 and 87% by the AuNPs-COOH and AuNPs-DMAP doping, respectively. Park and coauthors showed that binding of AuNPs on the surface of nanotubes containing pyrene molecules led to a drastic quenching of the pyrene emission to ca. 15% due to photoinduced electron transfer from the pyrene units to proximity of AuNPs.²⁴ Our small quenching should be attributed to the special structure of the PAH-Py NRs, on

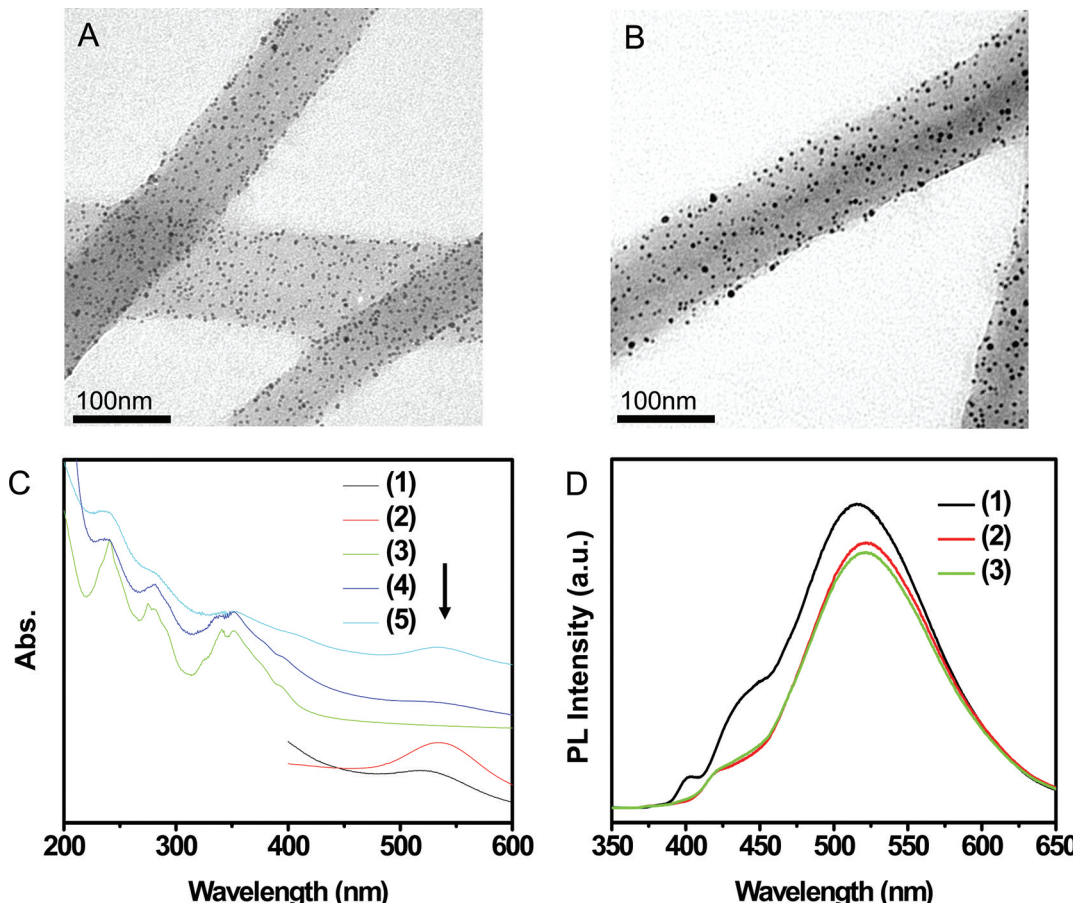


Figure 4. TEM images of (A) PAH-Py NRs with AuNP-COOH, (B) PAH-Py NRs with AuNP-DMAP. (C) UV-vis absorption spectra of (1) AuNP-COOH solution, (2) AuNP-DMAP solution, (3) PAH-Py NRs, (4) PAH-Py NRs with AuNP-COOH, and (5) PAH-Py NRs with AuNP-DMAP. (D) Fluorescence spectra of (1) PAH-Py NRs, (2) PAH-Py NRs with AuNP-COOH, and (3) PAH-Py NRs with AuNP-DMAP.

which the thick PAH layer (~ 45 nm) may avoid direct attachment of AuNPs to the pyrene units.

The second approach adsorbed directly the metal ions such as HAuCl_4 and K_2PtCl_4 , followed by reduction to obtain the metal nanoparticles decorated PAH-Py NRs. Formation of the metal NPs by this *in situ* reduction method has been well demonstrated on various particles and dendrimeric systems.^{36–38} In this work, the PAH-Py NRs were incubated in HAuCl_4 solution at room temperature for 2 days. During this process, the AuCl_4^- ions were reduced to AuNPs by the amino groups of PAH, as demonstrated previously by chitosan reduction.³⁶ The *in situ* synthesized AuNPs had a mean diameter of 47.7 ± 10.1 nm with a lower particle density (Figure 5A) because of a smaller number of seeds and a slower growth rate of gold crystal at lower temperature. When the incubation temperature increased to 80°C , the color of PAH-Py NRs solution changed from light yellow to wine red just within 1 h. In this case, the as-prepared AuNPs turned out to be smaller in size (mean diameter 12.5 ± 6.6 nm) with a higher density (Figure 5B), because a higher temperature promotes the formation of gold crystal seeds and growth. Formation of the AuNPs was also verified by EDX (see Figure S9 in the Supporting Information), which found the loading percentages of 22.1 and 26.7% for the larger and smaller AuNPs, respectively.

The generality of the *in situ* metal NP reduction was demonstrated by Pt NPs synthesis on the PAH-Py NRs (see Figure S10 in the Supporting Information). By adsorption of

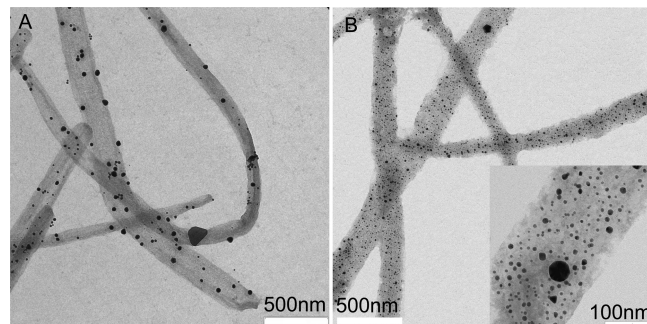


Figure 5. TEM images of PAH-Py NRs after incubated with HAuCl_4 (A) at 25°C for 2 days and (B) at 80°C for 1 h.

K_2PtCl_4 and following with reduction of cold NaBH_4 solution, PtNP clusters were formed on the PAH-Py NRs (Figure S10A), which showed a surface plasmon band around 390–400 nm (see Figure S10B in the Supporting Information). Their chemical structure was further confirmed by EDX analysis (see the Figure S10C in the Supporting Information).

The metal particles modified PAH-Py NRs could have great potential applications in many areas such as detection of chemicals, photothermal therapy, and catalysis. As shown in Figure 6, compared to the weak Raman bands for trans-azobenzoic acid adsorbed on the PAH-Py NRs, the bands at 1585 , 1410 , 1379 , 1352 , 1187 , and 1115 cm^{-1} for *trans*-

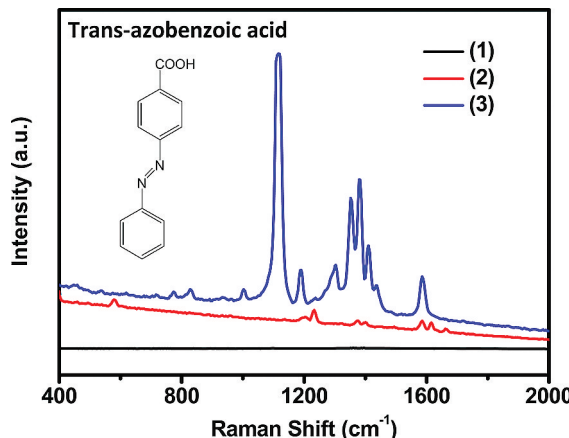


Figure 6. Raman spectra of (1) PAH-Py NRs; (2) PAH-Py NRs with trans-azobenzoic acid; (3) AuNP-modified PAH-Py NRs with trans-azobenzoic acid.

azobenzoic acid were strongly enhanced after AuNPs modification as a result of a well-known effect of SERS.³⁰

Previously, several methods were presented for controlling the coverage of gold nanoparticles onto surfaces comprised of organic molecules. Aggregates of nanoparticles were usually obtained regardless of the nanoparticles concentration.³⁹ The method described here provides a new approach for modification of organic surfaces with nanoparticles, resulting in multifunctional 1D organic nanostructures.

In conclusion, the PAH-Py NRs consisting of a Py-CHO core and PAH shell were successfully prepared by surface grafting of PAH onto Py-CHO NRs. They showed a more curved and flexible structure as a result of partial loss of Py-CHO from the NRs. Compared to the hydrophobic Py-CHO NRs, which were easily precipitated in water, the PAH-Py NRs with a hydrophilic and repulsive PAH layer could be suspended stably in water for at least 3 months. Because of the charge attraction and coordination effect of amino groups, AuNPs were successfully adsorbed onto the PAH-Py NRs surface or in situ synthesized after Au ions adsorption and reduction. Importantly, the initial fluorescence emission of Py was largely remained due to the excellent isolation effect of PAH, which avoids direct attachment between Py and the Au nanoparticles. Using the similar process, other hybrid organic-inorganic functional nanomaterials with controlled physical and chemical structures can also be prepared.

■ ASSOCIATED CONTENT

§ Supporting Information

Supporting spectroscopy and imaging data. This material is available free of charge via the Internet at <http://pubs.acs.org>.

■ AUTHOR INFORMATION

Corresponding Author

*E-mail: cygao@mail.hz.zj.cn. Tel/Fax: +86-571-87951108.

■ ACKNOWLEDGMENTS

Z.P.W. acknowledges the Max-Planck Society for a visiting grant. This work is financially supported by the Zhejiang Provincial Natural Science Foundation of China (Z4090177), the Ministry of Science and Technology of China for the Indo-China Cooperation (2010DFA51510) and the Natural Science Foundation of China (50873087).

■ REFERENCES

- (1) Zang, L.; Che, Y. K.; Moore, J. S. *Acc. Chem. Res.* **2008**, *41*, 1596.
- (2) Rao, C. N. R.; Govindaraj, A. *Adv. Mater.* **2009**, *21*, 4208.
- (3) Yuan, J. Y.; Muller, A. H. E. *Polymer* **2010**, *51*, 4015.
- (4) Hu, J. T.; Odom, T. W.; Lieber, C. M. *Acc. Chem. Res.* **1999**, *32*, 435.
- (5) Xia, Y. N.; Yang, P. D.; Sun, Y. G.; Wu, Y. Y.; Mayers, B.; Gates, B.; Yin, Y. D.; Kim, F.; Yan, Y. Q. *Adv. Mater.* **2003**, *15*, 353.
- (6) He, Q.; Cui, Y.; Ai, S. F.; Tian, Y.; Li, J. B. *Curr. Opin. Colloid Interface Sci.* **2009**, *14*, 115.
- (7) Hochbaum, A. I.; Yang, P. D. *Chem. Rev.* **2010**, *110*, 527.
- (8) Schmidt, V.; Wittemann, J. V.; Gosele, U. *Chem. Rev.* **2010**, *110*, 361.
- (9) Kim, H. C.; Park, S. M.; Hinsberg, W. D. *Chem. Rev.* **2010**, *110*, 146.
- (10) Habas, S. E.; Platt, H. A. S.; van Hest, M.; Ginley, D. S. *Chem. Rev.* **2010**, *110*, 6571.
- (11) Law, M.; Sirbuly, D. J.; Johnson, J. C.; Goldberger, J.; Saykally, R. J.; Yang, P. D. *Science* **2004**, *305*, 1269.
- (12) Johnson, J. C.; Choi, H. J.; Knutson, K. P.; Schaller, R. D.; Yang, P. D.; Saykally, R. J. *Nat. Mater.* **2002**, *1*, 106.
- (13) Wang, X. D.; Song, J. H.; Liu, J.; Wang, Z. L. *Science* **2007**, *316*, 102.
- (14) Wang, X. S.; Guerin, G.; Wang, H.; Wang, Y. S.; Manners, I.; Winnik, M. A. *Science* **2007**, *317*, 644.
- (15) Wang, X. S.; Liu, K.; Arsenault, A. C.; Rider, D. A.; Ozin, G. A.; Winnik, M. A.; Manners, I. *J. Am. Chem. Soc.* **2007**, *129*, 5630.
- (16) Stearns, L. A.; Chhabra, R.; Sharma, J.; Liu, Y.; Petuskey, W. T.; Yan, H.; Chaput, J. C. *Angew. Chem., Int. Ed.* **2009**, *48*, 8494.
- (17) Han, K. H.; Lee, E.; Kim, J. S.; Cho, B. K. *J. Am. Chem. Soc.* **2008**, *130*, 13858.
- (18) An, B. K.; Gihm, S. H.; Chung, J. W.; Park, C. R.; Kwon, S. K.; Park, S. Y. *J. Am. Chem. Soc.* **2009**, *131*, 3950.
- (19) Balakrishnan, K.; Datar, A.; Oitker, R.; Chen, H.; Zuo, J. M.; Zang, L. *J. Am. Chem. Soc.* **2005**, *127*, 10496.
- (20) Dong, H. L.; Jiang, S. D.; Jiang, L.; Liu, Y. L.; Li, H. X.; Hu, W. P.; Wang, E. J.; Yan, S. K.; Wei, Z. M.; Xu, W.; Gong, X. *J. Am. Chem. Soc.* **2009**, *131*, 17315.
- (21) Shao, H.; Parquette, J. R. *Angew. Chem., Int. Ed.* **2009**, *48*, 2525.
- (22) Hentschel, J.; Krause, E.; Borner, H. G. *J. Am. Chem. Soc.* **2006**, *128*, 7722.
- (23) Park, C.; Lee, I. H.; Lee, S.; Song, Y.; Rhue, M.; Kim, C. *Proc. Natl. Acad. Sci. U.S.A.* **2006**, *103*, 1199.
- (24) Park, C.; Im, M. S.; Lee, S.; Lim, J.; Kim, C. *Angew. Chem., Int. Ed.* **2008**, *47*, 9922.
- (25) Ai, S. F.; Lu, G.; He, Q.; Li, J. B. *J. Am. Chem. Soc.* **2003**, *125*, 11140.
- (26) Qu, X.; Komatsu, T. *Acs Nano* **2010**, *4*, 563.
- (27) Yuan, J. Y.; Xu, Y. Y.; Walther, A.; Bolisetty, S.; Schumacher, M.; Schmalz, H.; Ballauff, M.; Muller, A. H. E. *Nat. Mater.* **2008**, *7*, 718.
- (28) Yuan, J. Y.; Schacher, F.; Drechsler, M.; Hanisch, A.; Lu, Y.; Ballauff, M.; Muller, A. H. E. *Chem. Mater.* **2010**, *22*, 2626.
- (29) Wang, Z. P.; Moehwald, H.; Gao, C. Y. *ACS Nano* **2011**, *5*, 3930.
- (30) Stuart, C. M.; Frontiera, R. R.; Mathies, R. A. *J. Phys. Chem. A* **2007**, *111*, 12072.
- (31) Skirtach, A. G.; Karageorgiev, P.; Bedard, M. F.; Sukhorukov, G. B.; Moehwald, H. *J. Am. Chem. Soc.* **2008**, *130*, 11572.
- (32) Mei, Y.; Sharma, G.; Lu, Y.; Ballauff, M.; Drechsler, M.; Irrgang, T.; Kempe, R. *Langmuir* **2005**, *21*, 12229.
- (33) Lehn, J. M. *Chem. Soc. Rev.* **2007**, *36*, 151.
- (34) Gittins, D. I.; Caruso, F. *Angew. Chem., Int. Ed.* **2001**, *40*, 3001.
- (35) Volodkin, D. V.; Madabousi, N.; Blacklock, J.; Skirtach, A. G.; Mohwald, H. *Langmuir* **2009**, *25*, 14037.
- (36) Wang, B.; Chen, K.; Jiang, S.; Reincke, F.; Tong, W. J.; Wang, D. Y.; Gao, C. Y. *Biomacromolecules* **2006**, *7*, 1203.
- (37) Yuan, J.; Lu, Y.; Schacher, F.; Lunkenbein, T.; Weiss, S.; Schmalz, H.; Muller, A. H. E. *Chem. Mater.* **2009**, *21*, 4146.

(38) Garcia, M. E.; Baker, L. A.; Crooks, R. M. *Anal. Chem.* **1999**, *71*, 256.

(39) Skirtach, A. G.; Dejugnat, C.; Braun, D.; Susha, A. S.; Rogach, A. L.; Sukhorukov, G. B. *J. Phys. Chem. C* **2007**, *111*, 555.